Optical activation of TrkB neurotrophin receptor in mouse ventral hippocampus promotes plasticity and facilitates fear extinction

Juzoh Umemori[1§*], Giuliano Didio[1*], Frederike Winkel[1], Maria Llach Pou[1], Juliana Harkki[1], Giacomo Lo Russo[2], Maarten Verie[1], Hanna Antila[1], Chloe Buj[3], Tomi Taira[4], Sari E. Lauri[5], Ramon Guirado[6], Eero Castrén[1§]

1 Neuroscience Center, HiLIFE, University of Helsinki, Finland.
2 Department of Life Sciences, University of Trieste, Italy
3 Neurobiologie, Neurophysiologie, Neuropathologie, Aix-Marseille University, Master Neurosciences, France
4 Department of Veterinary Biosciences and Neuroscience Center, University of Helsinki, Finland
5 Molecular and Integrative Biosciences Research Programme, University of Helsinki, Finland
6 Neurobiology Unit, Department of Cell Biology, Interdisciplinary Research Structure for Biotechnology and Biomedicine (BIOTECMED), Universitat de Valencia, Spain.

* shared first author
§ shared corresponding author
Juzoh Umemori,
Neuroscience center, HiLife, University of Helsinki, 00790 Helsinki, Finland
Phone +358-45-1578-930
juzoh.umemori@helsinki.fi

Eero Castrén,
Neuroscience center, HiLife, University of Helsinki,
P.O.Box 63 (Biomedicum 1), 00014 Helsinki, Finland
Phone: +358-50 520 7974
eero.castren@helsinki.fi

Abstract

Successful extinction of traumatic memories depends on neuronal plasticity in the fear extinction network. However, the mechanisms involved in the extinction process remain poorly understood. Here, we investigated the fear extinction network by using a new optogenetic technique that allows temporal and spatial control of neuronal plasticity *in vivo*. We optimized an optically inducible TrkB (CKII-optoTrkB), the receptor of the brain-derived neurotrophic factor, which can be activated upon blue light exposure to increase plasticity specifically in pyramidal neurons. The activation of CKII-optoTrkB facilitated the induction of LTP in Schaffer collateral-CA1 synapses after brief theta-burst stimulation and increased the expression of FosB in the pyramidal neurons of the ventral hippocampus, indicating enhanced plasticity in that brain area. We showed that optical stimulation of the CA1 region of the ventral hippocampus during fear extinction training led to an attenuated conditioned fear memory. This was a specific effect only observed when combining extinction training with CKII-optoTrkB activation, and not when using either intervention alone. Thus, TrkB activation in ventral CA1 pyramidal neurons promotes a state of neuronal plasticity that allows extinction training to guide neuronal network remodeling to overcome fear memories. Our methodology is a powerful tool to induce neuronal network remodeling in the adult brain, and can attenuate neuropsychiatric symptoms caused by malfunctioning networks.

Introduction

Under pathological conditions, such as post-traumatic stress disorder (PTSD), phobias, and depression/anxiety disorders, traumatic memories are repeatedly and improperly retrieved (1,2). Exposure therapy, where the subject is repeatedly exposed to fear-inducing stimuli under safe conditions, is a widely used method to extinguish or suppress fear responses (3). Fear extinction has been successfully modeled in both humans and animals using the Pavlovian fear conditioning/extinction paradigm, where a neutral conditioned stimulus (CS, tone or context) starts to elicit a fear response after being associated with an aversive unconditioned stimulus (US). This fear response is reduced after a repeated exposure to the CS without the US (4–6). Although extinction training gradually reduces the fear responses in human patients and adult rodents, these fear responses tend to reappear with time or upon later re-exposure to the CS, a phenomena known as “spontaneous recovery”, and “fear renewal” when induced by a neutral cue or the same context, respectively (7,8). We have previously shown that the combination of extinction training and chronic treatment with fluoxetine, a commonly used antidepressant, but neither treatment alone, induces an enduring loss of conditioned fear memory in adult mice (9), which is similar to the permanent fear extinction found in early postnatal mice (10,11). A chronic treatment with fluoxetine reactivates a state of plasticity similar to that observed during the critical periods of plasticity or induced juvenile-like plasticity, a state we refer as iPlasticity, which have been shown in different brain regions, such as the amygdala, medial prefrontal cortex (mPFC), and hippocampus (9,12,13). These observations suggest that fear extinction is a process dependent on the reshaping of neural networks through experience-dependent plasticity. However, the mechanisms through which neural networks are reconfigured are still unknown.

Brain-derived neurotrophic factor (BDNF), through activation of its neurotrophic receptor tyrosine kinase B (TrkB), is thought to be a key factor in neuronal plasticity and required for the iPlasticity by fluoxetine treatment (9,14). The binding of BDNF to TrkB causes dimerization and autophosphorylation of TrkB, leading to activation of intracellular signaling pathways involved in neuronal differentiation, survival, and growth as well as synaptic plasticity in neurons (15,16). These pathways also regulate gene transcription and long-term potentiation (LTP) (17,18). Interestingly, Chang et al created a photoactivatable TrkB (optoTrkB), where full-length TrkB is conjugated with

a photolyase homology region (PHR) that dimerizes in response to blue light (470 nm) (19). They have shown that light stimulation can activate the canonical Trk signaling pathways through optoTrkB in a reversible manner, and a prolonged patterned stimulation induces differentiation of cultured neurons (19).

Here, we studied whether activation of TrkB through optoTrkB *in vivo* is sufficient to induce plasticity in the fear circuit and to facilitate fear extinction. For an efficient expression of optoTrkB in pyramidal neurons, we constructed a lentivirus that expresses optoTrkB (19) modified in the following points: (i) optimization of codons of the PHR domain for higher expression in rodents, (ii) attachment of a flexible tag (20) between TrkB and PHR, which allows a better interaction between optoTrkB C-terminus and its partners (21), and (iii) expression of a fusion protein by a short-type (0.4 kb) promoter of calcium/calmodulin-dependent protein kinase type II alpha subunit (CKII) for specific expression in pyramidal neurons (22). After confirming that CKII-optoTrkB lentivirus is expressed and activated in cultured cortical neurons, we activated CKII-optoTrkB in the projection neurons of the ventral hippocampus (vHP), which are known to be involved in fear extinction (23,24) through the modification of mood and spatial memory (25), and conducted the Pavlovian fear conditioning paradigm.

Material and Method

All animal experiments followed the Council of Europe guidelines and were approved by the State Provincial Office of Southern and Eastern Finland. Detailed procedures are described in the Supplementary Information.

Mice

C57BL/6JHss were originally purchased from Harlan (Netherlands); 10- to 12-week-old mice were used for this study. Mice were kept under standard laboratory conditions (21ºC, 12-h light-dark cycle, light at 6AM) with free access to food and water.

Infection of lentivirus and optic stimulation of optoTrkB in cultured cortical neurons

Rat primary cortical cultured neurons from E17 rat embryos were prepared using a method reported previously (26). The cells were infected with CKII-optoTrkB lentivirus (initial stock titer 8.37×10^7 pg/ml [p24]) at day *in vitro* 3 (DIV3) for immunoblotting, while the other cells on coverslips were infected at DIV9 for morphological analyses. The plates were kept in darkness at all time after the infections. The cells were exposed to blue light (LED devices, Mightex) at DIV10 and DIV17 for immunoblotting and immunocytology, respectively. The cells were photo-stimulated 12 times for 5 seconds with a 1-minute inter-trial interval, aiming to mimic the behavioral experiments. The cells were collected immediately for immunoblotting and 24 hours later for immunocytology. For immunoblotting, cells were lysed following a protocol described previously (27) and stored in darkness at -80°C. The samples for immunocytology were fixed with 4% of paraformaldehyde (PFA) and stored in PBS containing 0.02% NaN_3 at 4 °C.

Immunoblotting of lysate from cultured cells

Immunoblotting was conducted according to a method reported previously (27). Details on primary and secondary antibodies are provided in supplemental table 1. Chemiluminescent signals were developed by ECL plus (ThermoFisher Scientific) with a 5-minute incubation according to instructions provided by the manufacturer and detected by a LAS-3000 dark box (Fujifilm).

Imaging analyses on dendrites after immunocytology

We compared the number of spines in the secondary dendritic branches as described previously (28). All antibodies used for immunocytology are listed in supplemental table 1. The stained cells were imaged with a Leica TCS SP8 X with a magnification of 40x for analysis of primary neurites and spines. The primary branches sprouting from the soma were counted blindly and manually. Spines on the second branches were randomly and blindly selected. The number and type of spines were analyzed manually.

Lentivirus infection and implantation of optic cannulas

Mice were anesthetized with Isoflurane and fixed on a stereotactic frame. A total of 1 µl of virus solution was injected into the vHP, at 3.1 mm caudally and +/- 2.0 mm laterally from the Bregma with a depth of 3.9 mm and an angle of 18°. Three weeks after infection, optic fibers with cannula were inserted into the vHP, 3.1 mm caudally and +/- 3.0 mm laterally from the Bregma, with a depth of 3.0 mm and an angle of 4° and fixed and sealed with dental cement (Tetric Evo Flow). The mice were kept in single cages and underwent the fear conditioning/extinction test 1 week after the implantation.

Electrophysiology

Field excitatory postsynaptic potentials (fEPSP) were recorded in acute hippocampal slices. Briefly, the brains were isolated 4 weeks after infection with CKII-optoTrkB and immediately immersed in ice-cold dissection solution (29), after which 350-µm brain slices were cut and incubated for recovery for 45 minutes at 31 to 32°C in artificial cerebrospinal fluid (ACSF) (30). The slices were stimulated by light (LED 480 nm) three times for 5 seconds every minute. fEPSPs were then recorded in an interface chamber using ACSF-filled glass microelectrodes (2-4 MΩ) positioned within the CA1 stratum radiatum in response to Schaffer collateral stimulation (0.05 Hz). Stimulation intensity was adjusted such that the baseline fEPSP slope was 20-40% of the maximal intensity that resulted in the appearance of a population spike. LTP was subsequently induced by tetanus stimulation (100 pulses at 50 Hz) or brief theta-burst stimulation (1 episode of TBS consisting of 2 stimulus trains at 5 Hz with 4 pulses at 100 Hz).

Fear extinction test with optic stimulation

The fear conditioning paradigm was conducted following a protocol described previously (9). Briefly, the mice were put into Context A and received an electric foot shock (0.6 mA) after a 30-second sound cue ("beep" sounds 80 dB), which was repeated four times with a 30- to 60-second interval. Two days later the mice were put in Context B and received only the sound cue (30s "beep" sound 80 dB) immediately followed by optical stimulation for 5 seconds. The light was applied manually by a single-color LED (470nm wave length) device (Mightex) connected to a BioLED light source Control Module (Mightex), which in turn was connected to optic wires splitting into two parallel optic fibers (Kyocera Inc.) ending on both sides on the ferrules implanted in the head of the mouse. Mice were made able to move freely through a rotary joint (Mightex). The extinction training with light stimulation was repeated 12 times with different intervals (25-60 seconds) for 2 days. One week after, the mice were tested in Context B (spontaneous recovery) followed by exposure to Context A (fear renewal) with the same sound cue (presented 4 times/test) provided during conditioning and extinction. Spontaneous recovery and fear renewal were tested again 3 weeks later as an estimate of remote memory. The durations of freezing were measured as an index of conditioned fear.

Immunohistochemistry and image analysis on FosB intensity

Mice were infected with CKII-optoTrkB and we implanted optic cannulas into the vHP as described above. The vHP were exposed to light 12 times for 5 seconds after a 30-second sound with different intervals (25-60 seconds) in the same way as in the extinction training through optic cannulas for 2 days. Twenty-four hours after the last stimulation, the animals were perfused transcardially with PBS followed by 4% PFA in PBS. Isolated brains were post-fixed overnight and stored in PBS with 0.02% NaN_3 until cut on a vibratome (VT 1000E, Leica). Free-floating sections (40 µm) were processed for fluorescence immunohistochemistry following a protocol described previously (31) using the antibodies listed in supplemental table 1. Images were obtained with a Zeiss LSM 710 confocal microscope with a magnification of 20x. The intensity of delta FosB was analyzed by Fiji software (32).

Statistics

Biochemical data were analyzed by unpaired t-test following F-test. If standard deviation of the two groups were not equal, Welch's correction was applied. For comparisons of more than two groups, we used one-way ANOVA followed by Holm-Sidak's multiple comparisons test. Behavioral data was analyzed by two-way ANOVA, taking sessions and light exposure/non-exposure as independent factors, followed by Fisher's LSD test. All statistical analyses were performed using Prism 6 or 8 (GraphPad Software), and shown in supplemental table 3. A p-value <0.05 was considered statistically significant.

Results

Construction of CKII-optoTrkB

We optimized the codons of the PHR domain and the resulting Codon Adaptation Index (CAI) (33) was increased to 0.86 in the optimized codon, compared to 0.79 as in Chang's original PHR (Supplemental fig. 1). The homology of DNA sequences between our construct and the original optoTrkB was 78% (Supplemental fig. 2). The optimized PHR region, flexible tag (20), and full-length TrkB were sub-cloned into a lentivirus backbone vector with a short-type (0.4 kb) CaMKIIa promoter (pFCK(0.4)GW) (22). The CKII-optoTrkB construct was used for lentivirus production (see supplemental note).

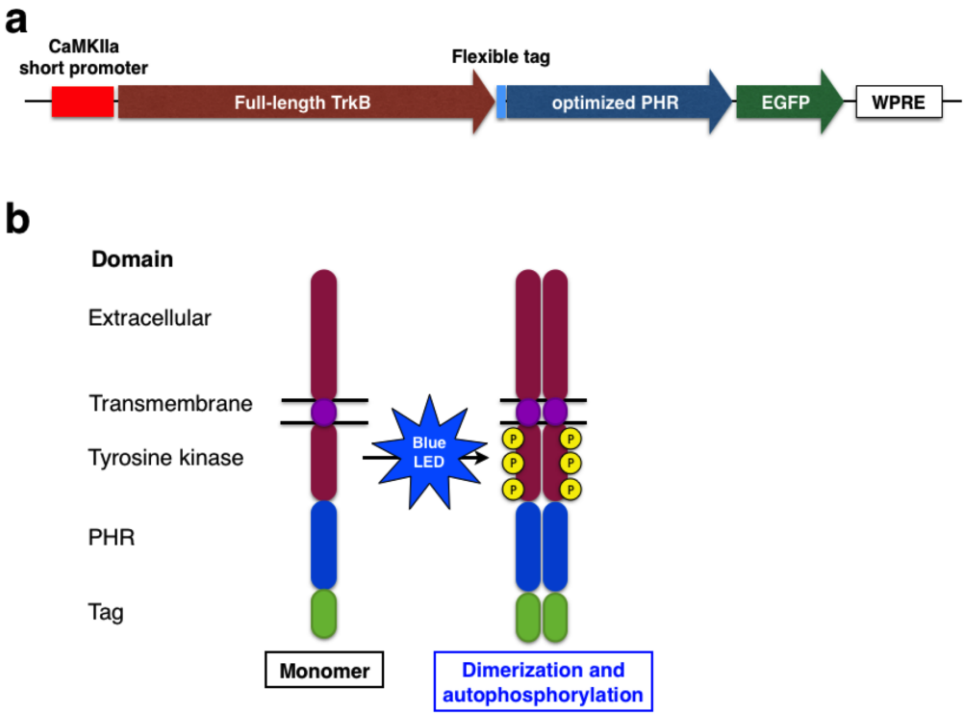

Figure 1 Development of optoTrkB for the *in vivo* study. (a) Gene structure of optoTrkB. CKII-optoTrkB consists of a short version (0.4 kb) of CaMKIIa promoter, full length TrkB, flexible tag, EGFP, and Woodchuck Hepatitis Virus (WHP) Posttranscriptional Regulatory Element (WPRE). (b) Protein structure of optoTrkB. TrkB consists of extracellular, transmembrane, and tyrosine kinase domains and was conjugates with PHR and GFP. The PHR domain dimerizes in response to blue light (470 nm) therefore inducing dimerization and autophosphorylation of TrkB to activate the canonical TrkB signaling pathways.

Optical stimulation of optoTrkB activates TrkB signals and neural plasticity in vitro

We determined the optimal virus concentration by testing different concentrations of CKII-optoTrkB in cultured cortical neurons and performed immunoblotting for phosphorylated TrkB (at tyrosine 706 residue, pY706), TrkB itself, and phosphorylated and non-phosphorylated Extracellular signal-regulated kinase (ERK), a downstream signal of the BDNF/TrkB pathway (Supplemental fig. 3). Immunoblotting with optimal concentration of the lentivirus showed an effect of light exposure on phosphorylation of optoTrkB at pY515, pY706, and pY816 (Fig. 2a, b, c, and d). As expected, phosphorylation of endogenous TrkB was not influenced by light (Supplemental fig. 4), but increased only after BDNF treatment (Supplemental fig. 5). Then we verified the phosphorylation of downstream signals of the BDNF/TrkB pathway and observed increased phosphorylation of cAMP response element-binding protein (CREB) and pERK after light stimulation when compared to the control group transfected with optoTrkB but not exposed to light (Fig. 2e, f).

To verify if the activation of optoTrkB causes morphological changes of dendrites and spines *in vitro*, we stained cortical primary neurons with MAP-2 antibody (Fig. 2g). The number of spines on second- and third-order dendritic branches was increased at 24 hours after light stimulation but not after BDNF treatment (5ng/ml) (Fig. 2h). Furthermore, we found an increased number of primary dendrites extending from the cell body in light-stimulated CKII-optoTrkB infected cells compared to non-stimulated cells or BDNF-treated cells. These results indicate that activation of optoTrkB promotes initial neurite and spine formation more rapidly than the BDNF treatment (28).

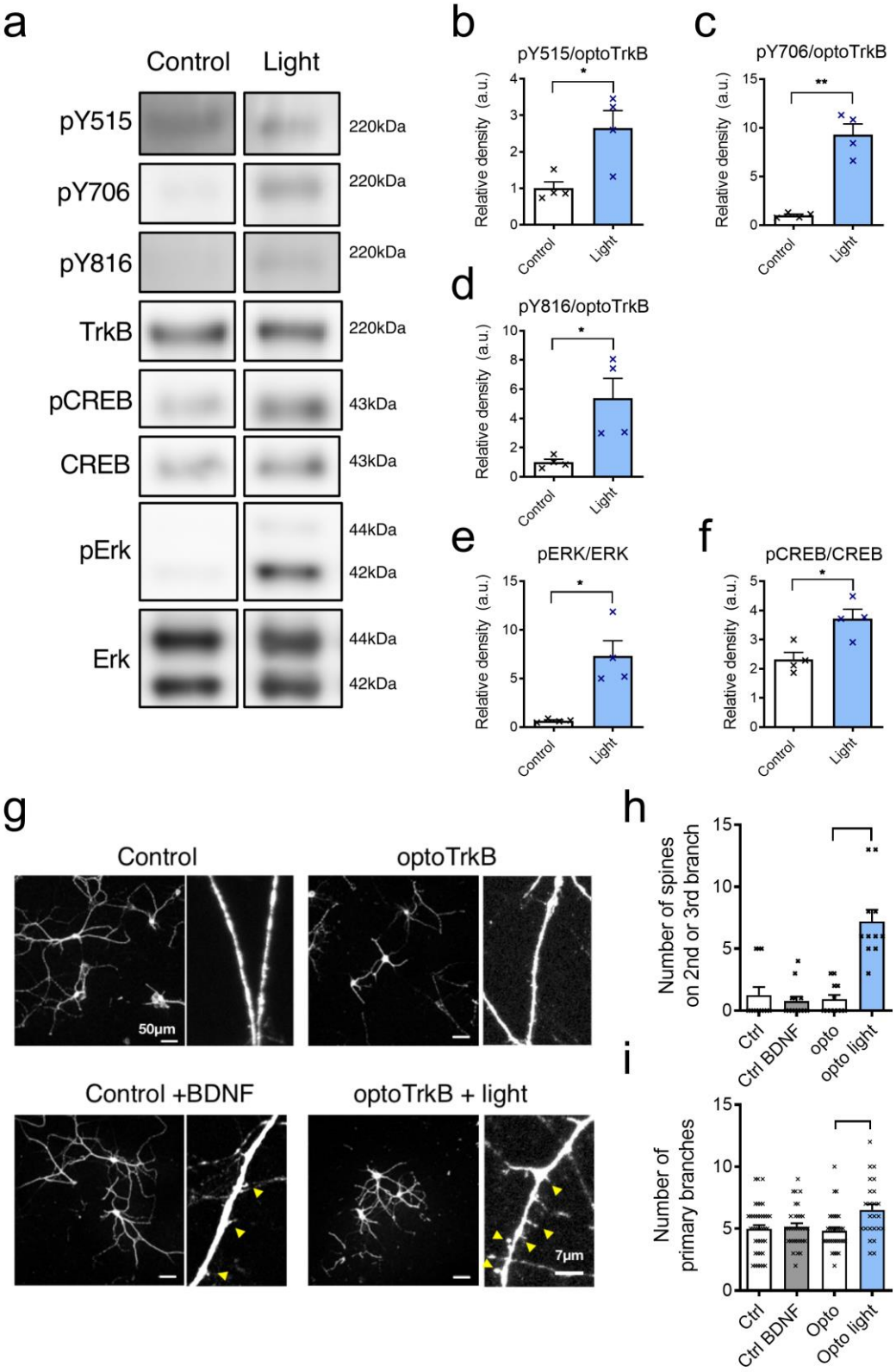

255

Figure 2 (a) Immunoblotting with antibodies against phosphorylated TrkB and downstream signals of TrkB. Quantitative analysis of phosphorylation of optoTrkB at pY515 (b), pY706 (c), and pY816 (d) phosphorylation site after light stimulation (12 times for 5 seconds with 1-minute interval) (N = 4, each group). The intensity of optoTrkB (220 kDa) was normalized with the non-phosphorylated version of the same protein. There were significant effects of light exposure on phosphorylation of optoTrkB at pY515 (unpaired t-test, $p = 0.0178$), pY706 ($p = 0.004$), and pY816 ($p = 0.0477$). Quantitative analysis of phosphorylation of ERK (e) and CREB (f) after light stimulation. Intensity of the bands of phosphorylated ERK (pERK) and CREB (pCREB) was normalized by non-phosphorylated ERK(42 kDa) and CREB(43 kDa) , respectively. The ratios significantly increased after light stimulation (unpaired t-test, pCREB/CREB, $p = 0.0133$; pERK/ERK, $p = 0.025$). (g-i) Effects of activation of CKII-optoTrkB on primary dendrites and spines in cultured cortical neurons (DIV17). The uninfected neurons were treated with 5 ng/ml of BDNF as control. The number of spines on 2nd or 3rd branch and primary dendrites extending from the cell body was counted manually. (g) Representative images of MAP2 immunostaining of cortical neurons. (h) The number of spines was not increased after a 5ng/ml BDNF treatment (Holm-Sidak's multiple comparisons test, Control vs Control + BDNF, $p = 0.6898$). However, the number of spines after activation of CKII-optoTrkB was significantly higher than non-activated infected cells (one-way ANOVA, $p < 0.0001$; Holm-Sidak's multiple comparisons, optoTrkB vs optoTrkB light, $p < 0.0001$ (N=11-13 in each group). (i) The number of primary dendrites was not increased after BDNF treatment (Holm-Sidak's multiple comparisons test, Control vs Control + BDNF, $p = 0.6898$). However, the number of spines after activation of CKII-optoTrkB was significantly higher than non-activated infected cells (one-way ANOVA, $p = 0.0053$; Holm-Sidak's multiple comparisons, optoTrkB vs optoTrkB light, $p = 0.0023$ (N=11-13 in each group).. (N = 48-63 in each group). CREB, cAMP response element-binding protein; ERK (Extracellular signal-regulated kinase). Scale bar, 50 µm. Bars represent means ± SEM. * $p < 0.05$, ** $p < 0.01$, *** $p < 0.001$.

Increased FosB expression after activation of optoTrkB in the ventral hippocampus

To confirm the activation of optoTrkB after light stimulation, optoTrkB lentivirus-infected mice were perfused 24 hours after 2 days of optic stimulation (12 sessions of 5-second exposure). Immunohistochemistry showed an increase of delta FosB expression in the regions close to the infection sites in the CA1 of the vHP (Fig. 3a and b), indicating that optoTrkB promotes BDNF/TrkB signals, as shown previously in case of overexpression of BDNF (34).

288 *LTP is potentiated after activation of optoTrkB*

289 To investigate synaptic plasticity in the hippocampal circuitry, fEPSPs were recorded in
290 acute hippocampal slices obtained from CMKII-optoTrkB lentivirus-infected mice after
291 *ex vivo* light stimulation. A traditional tetanus stimulation resulted in a comparable
292 induction of LTP in control and light-stimulated slices (Supplemental Fig. 6),
293 suggesting that a strong tetanization induces LTP independently from optoTrkB
294 activation. However, a brief theta-burst stimulation led to a robust increase in synaptic
295 strength only in light-stimulated slices (Fig. 3c), while it produced a slight potentiation
296 of fEPSPs in slices infected with optoTrkB without light exposure (control). This
297 indicates that the activation of CKII-optoTrkB facilitates LTP induced by a brief theta-
298 burst stimulation in the hippocampus.
299

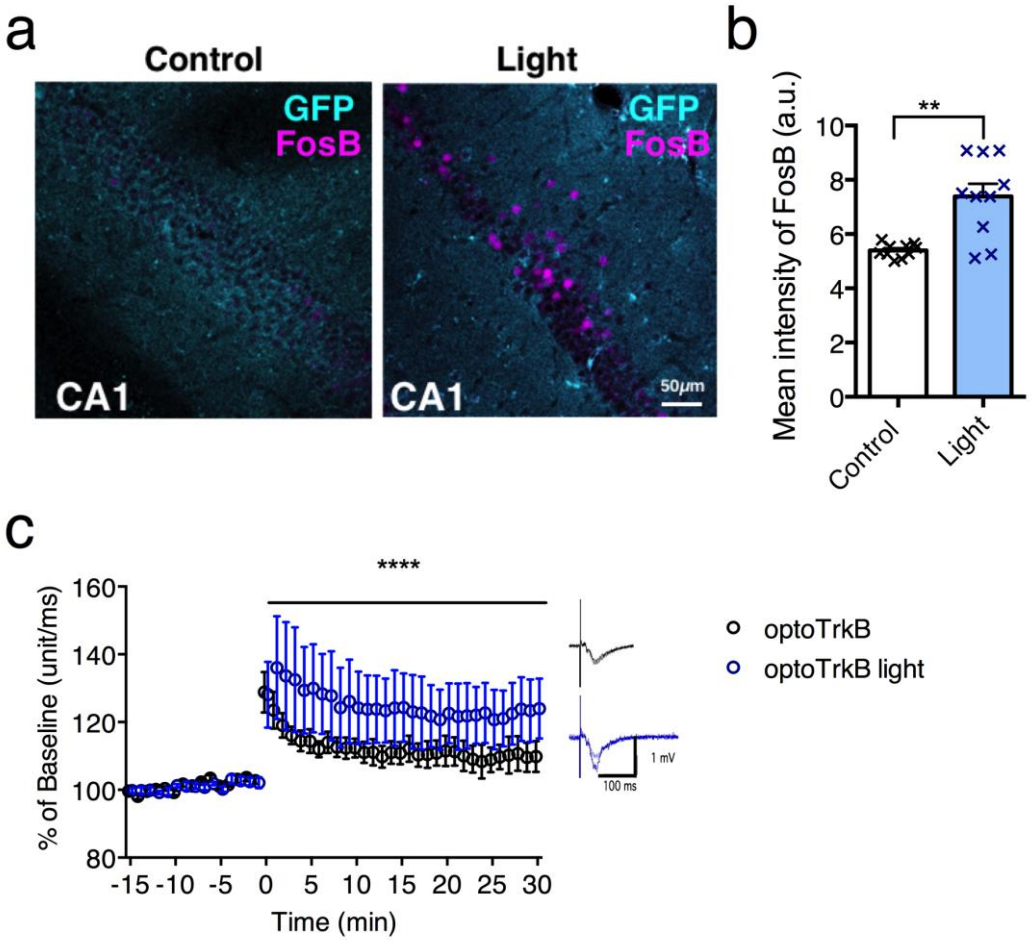

300
301

Figure 3 Enhanced neural plasticity after optoTrkB activation ex vivo. BDNF/TrkB signals were activated in the pyramidal neurons in the CA1 of the vHP after optic stimulation of CKII-optoTrkB. (a) Representative figures of the delta FosB and EGFP stainings close to the infection sites in the CA1of vHP. (b) Comparison of the intensity of delta FosB staining between non-light and light stimulation (N = 10, each group). Delta FosB immunoreactivity was higher in the group with light stimulation compared to the group without light stimulation (unpaired t-test, $p = 0.0006$). (c) The slices from CKII-optoTrkB infected mice were activated by light for 30 seconds. After 30 minutes, long-term potentiation (LTP) was induced by brief theta burst. fEPSPs during the last 10 minutes of recording were significantly larger in the group with light exposure compared to the group without light (two-way ANOVA, $p < 0.0001$). Pictures in the right panel show representative traces of fEPSC during baseline and after LTP induction. (optoTrkB, N = 5; optoTrkB light, N = 7). Error bars indicate mean ± SEM.

Activation of optoTrkB during fear extinction training reduces fear memory

Since the vHP is thought to be a key brain region for the processing of the extinction of contextual fear memory (23), we hypothesized that the activation of optoTrkB in the vHP during fear extinction may promote fear erasure. To test this hypothesis, we performed the fear conditioning paradigm (Fig. 4a). CKII-optoTrkB lentivirus was infected bilaterally into the CA1 region of the vHP, and optic cannulas were implanted into the same region (see Material and method) (Fig. 4b). During fear-conditioning/acquisition, all infected and implanted mice were conditioned by exposing them to a mild foot shock paired with a sound cue in context A, and all mice showed increased freezing (supplemental fig. 6). The mice were then equally divided into the following two groups: control (without stimulation) and light exposure (supplemental fig. 6). Two days later, the vHP was bilaterally exposed to light through optical fibers for 5 seconds immediately after the CS ("beep" sounds) in context B during 2 days of extinction training. During the extinction training of the first day (Ext1) (Fig. 4c) and the second day (Ext2) (Fig. 4d), both groups showed decreased freezing, but the effect was significantly more pronounced after LED stimulation. One week later there was no difference of freezing in context B (spontaneous recovery) and a weak decrease of the fear renewal in the LED group in context A (fear renewal) (supplemental fig. 7). However, three weeks later, the previously light-stimulated mice showed a decrease of freezing in the spontaneous recovery test (Fig. 4e) and a strong decrease in the fear renewal test (Fig. 4f). These results indicate that the light-stimulated mice initially retain a high freezing representation, but they then reduce the long-term or remote

334 contextual fear memory. CKII-optoTrkB-infected mice stimulated by light without
335 extinction training did not show differences compared to the control group during
336 remote spontaneous recovery (Fig. 4g) or remote fear renewal (Fig. 4h). On the
337 contrary, it was significantly different to the group exposed to both LED and extinction
338 training (Supplemental figure 7), indicating that conditioned fear is reduced only when
339 combining CKII-optoTrkB activation and extinction training but not with either
340 intervention alone.
341

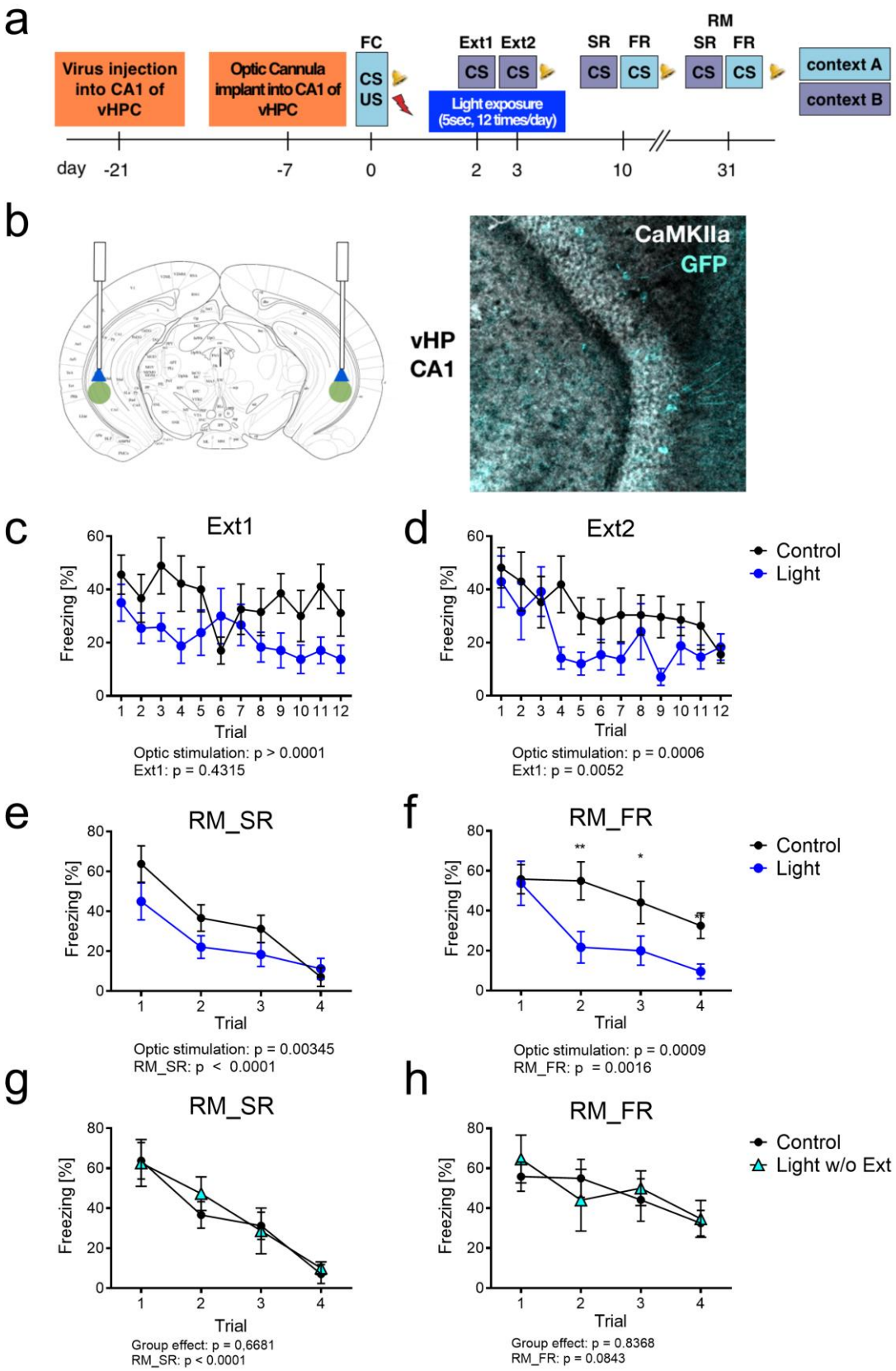

342

Figure 4 Activation of CKII-optoTrkB combined with extinction training promotes extinction of conditioned fear. (a) Scheme of fear extinction paradigm. Mice were subjected to fear extinction training in context B two days after fear conditioning with tones in context A. After 1 week, mice were then subjected to spontaneous recovery (SR) in context B and fear renewal (FR) in context A. Further 3 weeks later, the mice were subjected again to SR and FR for testing remote memory (RM). (b) CKII-optoTrkB lentivirus was infected into CA1 of the vHP (3.1 mm caudal, ±2 mm latera from Bregma, 3.9 mm depth from *dura mater*) (left). A representative infected site in the vHP (right). (c) (d) Significant effects of sessions were detected in freezing response during day 2 of extinction training (two-way ANOVA, $p = 0.0052$) and an effect of light stimulation during both days (Day1, $p < 0.0001$; Day2, $p = 0.0006$). In addition, there were significant differences between the first extinction session and the session with the lowest freezing duration post hoc (Fisher's LSD): control, 1st in 1st day vs 12th in 2nd, $p = 0.0060$; light, 1st in 1st day vs 9th in 2nd, $p = 0.0159$). Light-stimulated mice showed a decrease of freezing in remote spontaneous recovery (RM_SR) (two-way ANOVA: $p = 0.00345$) (e) and a strong decrease in remote fear renewal (RM_FR) ($p = 0.0009$) (f). Post-hoc analysis showed significant differences between two groups after second sessions (Fisher's LSD: light2-4, $p = 0.0002$; post-hoc: 2nd, $p = 0.0047$; 3rd, $p= 0.0362$; 4th, $p = 0.0465$). The group with light stimulation but no extinction training (LED w/o Ext) did not show decreased freezing during (g) remote spontaneous recovery (two-way ANOVA, $p = 0.6681$) or (h) remote fear renewal (two-way ANOVA, $p = 0.8368$) compared to control. Control (optoTrkB infected without light), N = 8, optoTrkB light, 8; optoTrkB light w/o extinction, 5). Error bars indicate mean ± SEM. * $p < 0.05$, ** $p < 0.01$.

Discussion

We developed a CKII-optoTrkB lentivirus by modifying the original optoTrkB (19) and demonstrated that it can be used to promote plasticity for *in vivo* studies. The optical activation of optoTrkB in the pyramidal neurons in the CA1 of the vHP promotes plasticity in the fear circuitry and enables fear extinction training to greatly reduce the conditioned fear memory, specifically the contextual memory. This study directly demonstrates that the activation of TrkB can promote plasticity-related behaviors in the fear circuitry. Moreover, our optoTrkB approach represents a new system to control plasticity temporarily and spatially.

Strong and rapid effects of optoTrkB activation compared to BDNF treatment

In cultured cortical neurons, light stimulation of CKII-optoTrkB promoted phosphorylation of CREB and ERK to the same extent as BDNF stimulation, suggesting that activation of CKII-optoTrkB has biochemically comparable effects to BDNF treatment at concentrations of 5 ng/ml. Moreover, in contrast to BDNF treatment, activation of optoTrkB promoted initial neurite and spine formation. It has been reported that a higher BDNF concentration is needed to observe such a drastic increase in the number of primary dendrites and spines (28,35,36). Thus, the activation of CKII-optoTrkB acts as rapidly and efficiently as longer treatment with high concentration of BDNF.

Neural plasticity is increased after activation of CKII-optoTrkB ex vivo

Previous studies with deleted and mutated TrkB showed impaired LTP at CA1 hippocampal synapses and impaired learning behaviors (15,18), indicating that TrkB activation is critical for LTP induction in the hippocampus. We now demonstrate that after direct activation of TrkB through CKII-optoTrkB a brief TBS produced a robust LTP that was significantly larger compared to controls. We used a modified and "brief" TBS, since a stronger TBS protocol robustly induces LTP in the hippocampus (37). Interestingly, induction of LTP in response to a strong tetanic stimulation was not affected by activation of CKII-optoTrkB, suggesting that TrkB activation lowered the threshold for LTP induction. Alternatively, LTP induced by tetanic stimulation could be reaching a "saturated point", occluding any facilitation by optoTrkB activation. TBS has been shown to reflect physiological conditions (38). Our results strongly suggest that

activation of optoTrkB can sensitize pyramidal neurons in the hippocampal network to be more plastic and to respond to a brief stimulation and adapt to external stimuli, such as an extinction training.

Activation of optoTrkB combined with extinction training reduces fear memory but does not delete it entirely.

In the current study, light-stimulated mice did not completely erase the fear response in the first session, but rather in the second session of the remote fear renewal tests. Similar effects, where fear response is decreased after the second session in fear renewal, were found after PNN removal in the basolateral amygdala (BA) before extinction training (11). In contrast, the combination of extinction training and chronic treatment with fluoxetine decreases the fear response almost completely even in the first session (9). These results suggest that optoTrkB activation in combination with extinction training does not completely replace or erase the conditioned fear memory but it reduces it by promoting neural plasticity in the pyramidal neuron network of vHP during the extinction training. These observations might support the idea that the original fear memory is preserved and the extinction training simply adds a new inhibitory association rather than erasing the original memory (39–41).

Fear extinction circuitry

Our results suggest that plasticity in pyramidal neurons in the vHP is a key element for processing the extinction of contextual fear memory. Fear extinction is thought to be controlled by a distributed network, including the amygdala, mPFC, and hippocampus (23). Prior evidence suggests that fear memories are disrupted with an increased activity of the vHC; optical activation of these neurons was reported to induce fear extinction and modification of behavior related to mood and spatial memory (25). The vHP may modulate emotional regulation, whereas dorsal HP is thought to contribute to cognitive functions such as learning and memory (42–46). The CA1 region of the vHP in particular sends strong projections to other regions, such as the BA, hypothalamus, nucleus accumbens, and the mPFC (47–50), and there is evidence that these projections process emotional behavior (51–53). In addition, impaired function in Hippocampal-prefrontal circuit has been observed in psychiatric patients including PTSD and schizophrenic subjects (54), and configurational changes in prefrontocortical

inputs from Amygdala and Hippocampus have been suggested as a possible mechanism underlying psychiatric disorders (55). Furthermore, it has been reported that BDNF infusion into the PFC and HP erases fear memory (56), and engram cells of projection neurons in CA1 of vHC play a necessary and sufficient role in social memory (57). Recently, Jimenez et al demonstrated that optogenetic activation of the CA1 terminals in BA impaired contextual fear memory (53). Thus, our results suggest that plastic changes in the projection neurons in CA1 of the vHP, enabled by optoTrkB activation, modify anxiogenic contextual information when combined with fear extinction training.

iPlasticity and application of optoTrkB system in vivo

Many kinds of interventions induce iPlasticity, where networks in adult brain are allowed to better adapt to the changes in the internal and external milieu (16,17,58). In addition to fear extinction, specific training and other external manipulations, when combined with fluoxetine, have been shown to increases neural plasticity and alter symptoms of neuropsychiatric diseases in models such as ocular dominance plasticity (14) and socialization animal models (59). We hypothesize that these effects are modulated via the BDNF/TrkB pathway, but it is not yet clear which neural pathways are modified through iPlasticity in these behaviors. OptoTrkB is a new tool for controlling neural plasticity in a temporal and cell-type specific manner and the optic control of neural plasticity adds another dimension to traditional optogenetics using direct activation and inhibition of neurons by channelrhodopsin and halorhodopsin in experimental neurosciences.

ACKNOWLEDGMENTS

We thank Sulo Kolehmainen and Outi Nikkila for assistance in all experiments. We also thank caretakers in the F-building in UH for assistance with animal care, and Lakovos Lazaridis and Konstantinos Meletis in the Karolinska institute for kindly providing instruction in optogenetic techniques. The original research in our laboratory was supported by the ERC grant # 322742 – iPLASTICITY, the Sigrid Jusélius foundation, the EU Joint Programme–Neurodegenerative Disease Research (JPND) project # JPCOFUND_FP-829-007, the HiLife Fellows program, the Academy of Finland grants #294710, 303124, and 307416, Bilateral exchange program between the Academy of

Finland and JSPS (Japan Society for the Promotion of Science), the Brain & Mind grants, and the University of Helsinki Research Foundation.

Conflict of Interest

The authors declare no competing financial interests.

AUTHOR CONTRIBUTIONS

J.U., R.G., and E.C. conceived of and designed the project. J.H., G.D., G.L., MV, and J.U. performed experiments related to cultured cells. M.L., H.A., G.D, F.W., and J.U. conducted operations, behavioral experiments, and immunohistochemistry. F.W. performed electrophysiological experiments under the supervision of T.T. and S.L. All authors were involved in writing the manuscript.

References

1. Jovanovic T, Ressler KJ. How the Neurocircuitry and Genetics of Fear Inhibition May Inform Our Understanding of PTSD. Am J Psychiatry [Internet]. 2010 Jun 1 [cited 2019 Jun 28];167(6):648–62. Available from: http://psychiatryonline.org/doi/abs/10.1176/appi.ajp.2009.09071074
2. Kheirbek MA, Klemenhagen KC, Sahay A, Hen R. Neurogenesis and generalization: a new approach to stratify and treat anxiety disorders. Nat Neurosci [Internet]. 2012 Dec 27 [cited 2019 Jun 28];15(12):1613–20. Available from: http://www.nature.com/articles/nn.3262
3. Bisson J, Andrew M. Psychological treatment of post-traumatic stress disorder (PTSD). In: Bisson J, editor. Cochrane Database of Systematic Reviews [Internet]. Chichester, UK: John Wiley & Sons, Ltd; 2007 [cited 2019 Jun 28]. Available from: http://doi.wiley.com/10.1002/14651858.CD003388.pub3
4. Milad MR, Rauch SL, Pitman RK, Quirk GJ. Fear extinction in rats: Implications for human brain imaging and anxiety disorders. Biol Psychol [Internet]. 2006 Jul 1 [cited 2019 Jun 28];73(1):61–71. Available from: https://www.sciencedirect.com/science/article/pii/S0301051106000263?via%3Dihub
5. LeDoux JE. Emotion Circuits in the Brain. Annu Rev Neurosci [Internet]. 2000 Mar 28 [cited 2019 Jun 28];23(1):155–84. Available from:

http://www.annualreviews.org/doi/10.1146/annurev.neuro.23.1.155

6. Mahan AL, Ressler KJ. Fear conditioning, synaptic plasticity and the amygdala: implications for posttraumatic stress disorder. Trends Neurosci [Internet]. 2012 Jan 1 [cited 2019 Jun 28];35(1):24–35. Available from: https://www.sciencedirect.com/science/article/pii/S0166223611001032?via%3Dihub

7. Yehuda R, LeDoux J. Response Variation following Trauma: A Translational Neuroscience Approach to Understanding PTSD. Neuron [Internet]. 2007 Oct 4 [cited 2019 Jun 28];56(1):19–32. Available from: https://www.sciencedirect.com/science/article/pii/S0896627307007040?via%3Dihub

8. Quirk GJ, Mueller D. Neural Mechanisms of Extinction Learning and Retrieval. Neuropsychopharmacology [Internet]. 2008 Jan 19 [cited 2019 Jun 28];33(1):56–72. Available from: http://www.nature.com/articles/1301555

9. Karpova NN, Pickenhagen A, Lindholm J, Tiraboschi E, Kulesskaya N, Ágústsdóttir A, et al. Fear erasure in mice requires synergy between antidepressant drugs and extinction training. Science (80-). 2011;334(6063):1731–4.

10. Kim JH, Richardson R. New Findings on Extinction of Conditioned Fear Early in Development: Theoretical and Clinical Implications. Biol Psychiatry [Internet]. 2010 Feb 15 [cited 2019 Jun 28];67(4):297–303. Available from: https://www.sciencedirect.com/science/article/pii/S0006322309010555?via%3Dihub

11. Gogolla N, Caroni P, Lüthi A, Herry C. Perineuronal nets protect fear memories from erasure. Science (80-). 2009;325(5945):1258–61.

12. Ohira K, Takeuchi R, Shoji H, Miyakawa T. Fluoxetine-induced cortical adult neurogenesis. Neuropsychopharmacology [Internet]. 2013;38(6):909–20. Available from: http://dx.doi.org/10.1038/npp.2013.2

13. Guirado R, Perez-Rando M, Sanchez-Matarredona D, Castrén E, Nacher J. Chronic fluoxetine treatment alters the structure, connectivity and plasticity of cortical interneurons. Int J Neuropsychopharmacol [Internet]. 2014;17(10):1635–46. Available from: https://academic.oup.com/ijnp/article-lookup/doi/10.1017/S1461145714000406

526 14. Vetencourt JFM, Sale A, Viegi A, Baroncelli L, De Pasquale R, O'leary OF, et
527 al. The antidepressant fluoxetine restores plasticity in the adult visual cortex.
528 Science (80-). 2008;320(5874):385–8.
529 15. Minichiello L, Calella AM, Medina DL, Bonhoeffer T, Klein R, Korte M.
530 Mechanism of TrkB-mediated hippocampal long-term potentiation. Neuron
531 [Internet]. 2002 Sep 26 [cited 2019 Jun 30];36(1):121–37. Available from:
532 http://www.ncbi.nlm.nih.gov/pubmed/12367511
533 16. Castrén E, Antila H. Neuronal plasticity and neurotrophic factors in drug
534 responses. Mol Psychiatry [Internet]. 2017 Aug 11 [cited 2017 Nov
535 24];22(8):1085–95. Available from:
536 http://www.nature.com/doifinder/10.1038/mp.2017.61
537 17. Castrén E. Is mood chemistry? Nat Rev Neurosci. 2005;6(3):241.
538 18. Minichiello L. TrkB signalling pathways in LTP and learning. Nat Rev Neurosci
539 [Internet]. 2009 Dec 1 [cited 2018 Jun 8];10(12):850–60. Available from:
540 http://www.nature.com/articles/nrn2738
541 19. Chang K-Y, Woo D, Jung H, Lee S, Kim S, Won J, et al. Light-inducible
542 receptor tyrosine kinases that regulate neurotrophin signalling. Nat Commun.
543 2014;5.
544 20. Kennedy MJ, Hughes RM, Peteya LA, Schwartz JW, Ehlers MD, Tucker CL.
545 Rapid blue-light–mediated induction of protein interactions in living cells. Nat
546 Methods [Internet]. 2010 Dec 31 [cited 2019 Jun 28];7(12):973–5. Available
547 from: http://www.nature.com/articles/nmeth.1524
548 21. Chen X, Zaro JL, Shen W-C. Fusion protein linkers: Property, design and
549 functionality. Adv Drug Deliv Rev [Internet]. 2013 Oct 15 [cited 2019 Jun
550 28];65(10):1357–69. Available from:
551 https://www.sciencedirect.com/science/article/pii/S0169409X12003006?via%3D
552 ihub
553 22. Dittgen T, Nimmerjahn A, Komai S, Licznerski P, Waters J, Margrie TW, et al.
554 Lentivirus-based genetic manipulations of cortical neurons and their optical and
555 electrophysiological monitoring in vivo. Proc Natl Acad Sci U S A [Internet].
556 2004 Dec 28 [cited 2019 Jun 28];101(52):18206–11. Available from:
557 http://www.ncbi.nlm.nih.gov/pubmed/15608064
558 23. Tovote P, Fadok JP, Lüthi A. Neuronal circuits for fear and anxiety. Nat Rev

559 Neurosci [Internet]. 2015 Jun 20 [cited 2019 Jun 28];16(6):317–31. Available
560 from: http://www.nature.com/articles/nrn3945
561 24. Sotres-Bayon F, Sierra-Mercado D, Pardilla-Delgado E, Quirk GJ. Gating of Fear
562 in Prelimbic Cortex by Hippocampal and Amygdala Inputs. Neuron [Internet].
563 2012 Nov 21 [cited 2019 Jun 28];76(4):804–12. Available from:
564 https://www.sciencedirect.com/science/article/pii/S0896627312008811?via%3Di
565 hub
566 25. Kheirbek MA, Drew LJ, Burghardt NS, Costantini DO, Tannenholz L, Ahmari
567 SE, et al. Differential Control of Learning and Anxiety along the Dorsoventral
568 Axis of the Dentate Gyrus. Neuron [Internet]. 2013 Mar 6 [cited 2019 Apr
569 21];77(5):955–68. Available from:
570 https://www.sciencedirect.com/science/article/pii/S0896627313000469?via%3Di
571 hub
572 26. Sahu MP, Nikkilä O, Lågas S, Kolehmainen S, Castrén E. Culturing primary
573 neurons from rat hippocampus and cortex. Neuronal Signal [Internet]. 2019 Jun
574 28 [cited 2019 Jul 7];3(2):NS20180207. Available from:
575 http://www.neuronalsignaling.org/lookup/doi/10.1042/NS20180207
576 27. Antila H, Ryazantseva M, Popova D, Sipilä P, Guirado R, Kohtala S, et al.
577 Isoflurane produces antidepressant effects and induces TrkB signaling in rodents.
578 Sci Rep [Internet]. 2017 Dec 10 [cited 2019 Jul 7];7(1):7811. Available from:
579 http://www.nature.com/articles/s41598-017-08166-9
580 28. Koshimizu H, Kiyosue K, Hara T, Hazama S, Suzuki S, Uegaki K, et al. Multiple
581 functions of precursor BDNF to CNS neurons: negative regulation of neurite
582 growth, spine formation and cell survival. Mol Brain [Internet]. 2009 Aug 13
583 [cited 2019 Jun 30];2(1):27. Available from:
584 http://molecularbrain.biomedcentral.com/articles/10.1186/1756-6606-2-27
585 29. Lauri SE, Segerstråle M, Vesikansa A, Maingret F, Mulle C, Collingridge GL, et
586 al. Journal of Neuroscience. J Neurosci [Internet]. 2005 May 4 [cited 2019 Aug
587 16];20(22):8269–78. Available from:
588 https://www.jneurosci.org/content/25/18/4473.long
589 30. Ting JT, Daigle TL, Chen Q, Feng G. Acute Brain Slice Methods for Adult and
590 Aging Animals: Application of Targeted Patch Clamp Analysis and
591 Optogenetics. In Humana Press, New York, NY; 2014 [cited 2019 May 24]. p.

221–42. Available from: http://link.springer.com/10.1007/978-1-4939-1096-0_14

31. Guirado R, Umemori J, Sipila P, Castren E. Evidence for Competition for Target Innervation in the Medial Prefrontal Cortex. Cereb Cortex [Internet]. 2016; Available from: http://www.scopus.com/inward/record.url?eid=2-s2.0-84961248410&partnerID=MN8TOARS

32. Schindelin J, Arganda-Carreras I, Frise E, Kaynig V, Longair M, Pietzsch T, et al. Fiji: an open-source platform for biological-image analysis. Nat Methods [Internet]. 2012 Jul 28 [cited 2019 Jul 7];9(7):676–82. Available from: http://www.nature.com/articles/nmeth.2019

33. Sharp PM, Li W-H. The codon adaptation index-a measure of directional synonymous codon usage bias, and its potential applications. Nucleic Acids Res [Internet]. 1987 Feb 11 [cited 2019 Jul 7];15(3):1281–95. Available from: https://academic.oup.com/nar/article-lookup/doi/10.1093/nar/15.3.1281

34. Wang J, Fanous S, Terwilliger EF, Bass CE, Hammer RP, Nikulina EM. BDNF Overexpression in the Ventral Tegmental Area Prolongs Social Defeat Stress-induced Cross-Sensitization to Amphetamine and Increases ΔFosB Expression in Mesocorticolimbic Regions of Rats. Neuropsychopharmacology [Internet]. 2013 Oct 21 [cited 2019 Aug 21];38(11):2286–96. Available from: http://www.nature.com/articles/npp2013130

35. Sato Y, Suzuki S, Kitabatake M, Hara T, Kojima M. Generation of TrkA/TrkB Chimeric Receptor Constructs Reveals Molecular Mechanisms Underlying BDNF-Induced Dendritic Outgrowth in Hippocampal Neurons. Cell Mol Neurobiol [Internet]. 2011 May 30 [cited 2019 Jul 7];31(4):605–14. Available from: http://link.springer.com/10.1007/s10571-011-9655-8

36. Ji Y, Pang PT, Feng L, Lu B. Cyclic AMP controls BDNF-induced TrkB phosphorylation and dendritic spine formation in mature hippocampal neurons. Nat Neurosci [Internet]. 2005 Feb 23 [cited 2021 Feb 4];8(2):164–72. Available from: http://www.nature.com/natureneuroscience

37. Nguyen P V, Kandel ER. Brief theta-burst stimulation induces a transcription-dependent late phase of LTP requiring cAMP in area CA1 of the mouse hippocampus. Learn Mem [Internet]. 1997 Jul 1 [cited 2019 Jul 7];4(2):230–43. Available from: http://www.ncbi.nlm.nih.gov/pubmed/10456066

38. Larson J, Munkácsy E. Theta-burst LTP. Brain Res [Internet]. 2015 Sep 24 [cited

2019 Jul 3];1621:38–50. Available from: https://www.sciencedirect.com/science/article/pii/S000689931401436X?via%3Dihub

39. Bouton ME, Westbrook RF, Corcoran KA, Maren S. Contextual and Temporal Modulation of Extinction: Behavioral and Biological Mechanisms. Biol Psychiatry [Internet]. 2006 Aug 15 [cited 2019 Jul 3];60(4):352–60. Available from: https://www.sciencedirect.com/science/article/pii/S0006322306000990?via%3Dihub

40. Quirk GJ. Memory for extinction of conditioned fear is long-lasting and persists following spontaneous recovery. Learn Mem [Internet]. 2002 Nov 1 [cited 2019 Jul 3];9(6):402–7. Available from: http://www.ncbi.nlm.nih.gov/pubmed/12464700

41. Schiller D, Cain CK, Curley NG, Schwartz JS, Stern SA, Ledoux JE, et al. Evidence for recovery of fear following immediate extinction in rats and humans. Learn Mem [Internet]. 2008 Jun 1 [cited 2019 Jul 3];15(6):394–402. Available from: http://www.ncbi.nlm.nih.gov/pubmed/18509113

42. Fanselow MS, Dong H-W. Are the Dorsal and Ventral Hippocampus Functionally Distinct Structures? Neuron [Internet]. 2010 Jan 14 [cited 2019 Apr 18];65(1):7–19. Available from: https://www.sciencedirect.com/science/article/pii/S0896627309009477?via%3Dihub

43. Strange BA, Witter MP, Lein ES, Moser EI. Functional organization of the hippocampal longitudinal axis. Nat Rev Neurosci [Internet]. 2014 Oct 19 [cited 2019 Jul 7];15(10):655–69. Available from: http://www.nature.com/articles/nrn3785

44. Kjelstrup KG, Tuvnes FA, Steffenach H-A, Murison R, Moser EI, Moser M-B. Reduced fear expression after lesions of the ventral hippocampus. Proc Natl Acad Sci [Internet]. 2002 Aug 6 [cited 2019 May 1];99(16):10825–30. Available from: https://www.pnas.org/content/99/16/10825

45. Moser MB, Moser EI, Forrest E, Andersen P, Morris RG. Spatial learning with a minislab in the dorsal hippocampus. Proc Natl Acad Sci U S A [Internet]. 1995 Oct 10 [cited 2019 Jul 7];92(21):9697–701. Available from:

http://www.ncbi.nlm.nih.gov/pubmed/7568200

46. Bannerman DM, Sprengel R, Sanderson DJ, McHugh SB, Rawlins JNP, Monyer H, et al. Hippocampal synaptic plasticity, spatial memory and anxiety. Nat Rev Neurosci [Internet]. 2014 Mar 20 [cited 2019 May 1];15(3):181–92. Available from: http://www.nature.com/articles/nrn3677

47. Hoover WB, Vertes RP. Anatomical analysis of afferent projections to the medial prefrontal cortex in the rat. Brain Struct Funct [Internet]. 2007 Sep 10 [cited 2019 Apr 17];212(2):149–79. Available from: http://link.springer.com/10.1007/s00429-007-0150-4

48. Canteras NS, Swanson LW. Projections of the ventral subiculum to the amygdala, septum, and hypothalamus: A PHAL anterograde tract-tracing study in the rat. J Comp Neurol [Internet]. 1992 Oct 8 [cited 2019 Apr 17];324(2):180–94. Available from: http://doi.wiley.com/10.1002/cne.903240204

49. Cenquizca LA, Swanson LW. Spatial organization of direct hippocampal field CA1 axonal projections to the rest of the cerebral cortex. Brain Res Rev [Internet]. 2007 Nov 1 [cited 2019 Jul 7];56(1):1–26. Available from: https://www.sciencedirect.com/science/article/pii/S0165017307000732?via%3Dihub

50. Kishi T, Tsumori T, Yokota S, Yasui Y. Topographical projection from the hippocampal formation to the amygdala: A combined anterograde and retrograde tracing study in the rat. J Comp Neurol [Internet]. 2006 May 20 [cited 2019 Jul 7];496(3):349–68. Available from: http://doi.wiley.com/10.1002/cne.20919

51. Herry C, Ciocchi S, Senn V, Demmou L, Müller C, Lüthi A. Switching on and off fear by distinct neuronal circuits. Nature [Internet]. 2008 Jul 9 [cited 2019 Jul 7];454(7204):600–6. Available from: http://www.nature.com/articles/nature07166

52. Tannenholz L, Jimenez JC, Kheirbek MA. Local and regional heterogeneity underlying hippocampal modulation of cognition and mood. Front Behav Neurosci [Internet]. 2014 May 6 [cited 2019 Jul 7];8:147. Available from: http://journal.frontiersin.org/article/10.3389/fnbeh.2014.00147/abstract

53. Jimenez JC, Su K, Goldberg AR, Luna VM, Biane JS, Ordek G, et al. Anxiety Cells in a Hippocampal-Hypothalamic Circuit. Neuron [Internet]. 2018 Feb 7 [cited 2019 May 1];97(3):670-683.e6. Available from:

http://www.ncbi.nlm.nih.gov/pubmed/29397273

54. Godsil BP, Kiss JP, Spedding M, Jay TM. The hippocampal–prefrontal pathway: The weak link in psychiatric disorders? Eur Neuropsychopharmacol [Internet]. 2013 Oct 1 [cited 2019 May 6];23(10):1165–81. Available from: https://www.sciencedirect.com/science/article/pii/S0924977X12003136?via%3Dihub

55. Guirado R, Perez-Rando M, Ferragud A, Gutierrez-Castellanos N, Umemori J, Carceller H, et al. A Critical Period for Prefrontal Network Configurations Underlying Psychiatric Disorders and Addiction [Internet]. Vol. 14, Frontiers in Behavioral Neuroscience. Frontiers Media S.A.; 2020 [cited 2021 Feb 10]. p. 51. Available from: www.frontiersin.org

56. Peters J, Dieppa-Perea LM, Melendez LM, Quirk GJ. Induction of fear extinction with hippocampal-infralimbic BDNF. Science [Internet]. 2010 Jun 4 [cited 2019 Apr 24];328(5983):1288–90. Available from: http://www.ncbi.nlm.nih.gov/pubmed/20522777

57. Okuyama T, Kitamura T, Roy DS, Itohara S, Tonegawa S. Ventral CA1 neurons store social memory. Science [Internet]. 2016 Sep 30 [cited 2019 May 2];353(6307):1536–41. Available from: http://www.ncbi.nlm.nih.gov/pubmed/27708103

58. Umemori J, Winkel F, Didio G, Llach Pou M, Castrén E. iPlasticity: Induced juvenile-like plasticity in the adult brain as a mechanism of antidepressants. Psychiatry Clin Neurosci [Internet]. 2018 Sep 1 [cited 2018 Sep 14];72(9):633–53. Available from: http://doi.wiley.com/10.1111/pcn.12683

59. Mikics É, Guirado R, Umemori J, Tóth M, Biró L, Miskolczi C, et al. Social Learning Requires Plasticity Enhanced by Fluoxetine Through Prefrontal Bdnf-TrkB Signaling to Limit Aggression Induced by Post-Weaning Social Isolation. Neuropsychopharmacology [Internet]. 2017;1–11. Available from: http://www.nature.com/doifinder/10.1038/npp.2017.142

Supplemental figures

Supplemental Fig. 1

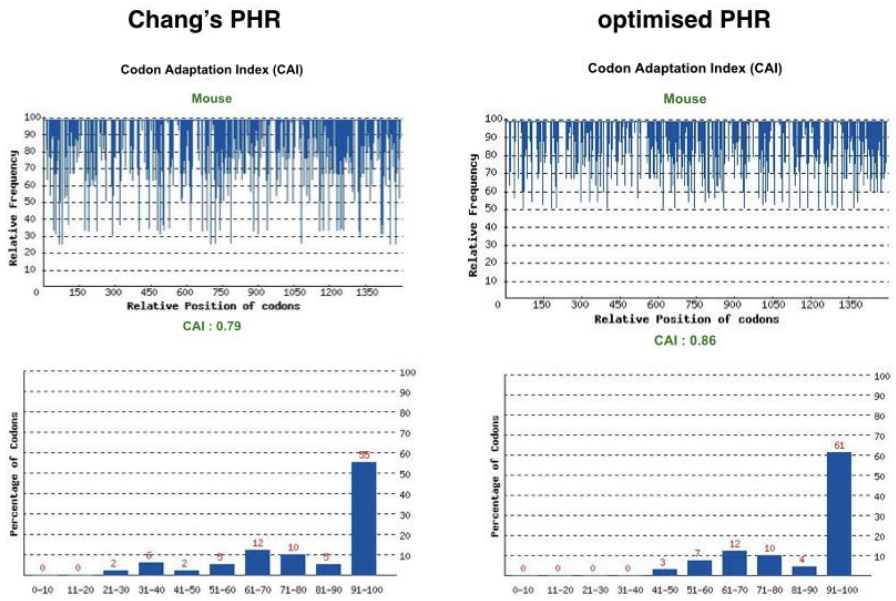

The percentage distribution of codons in computed codon quality groups

Supplemental Figure 1 optimized codons of PHR domain

Supplemental Fig. 2

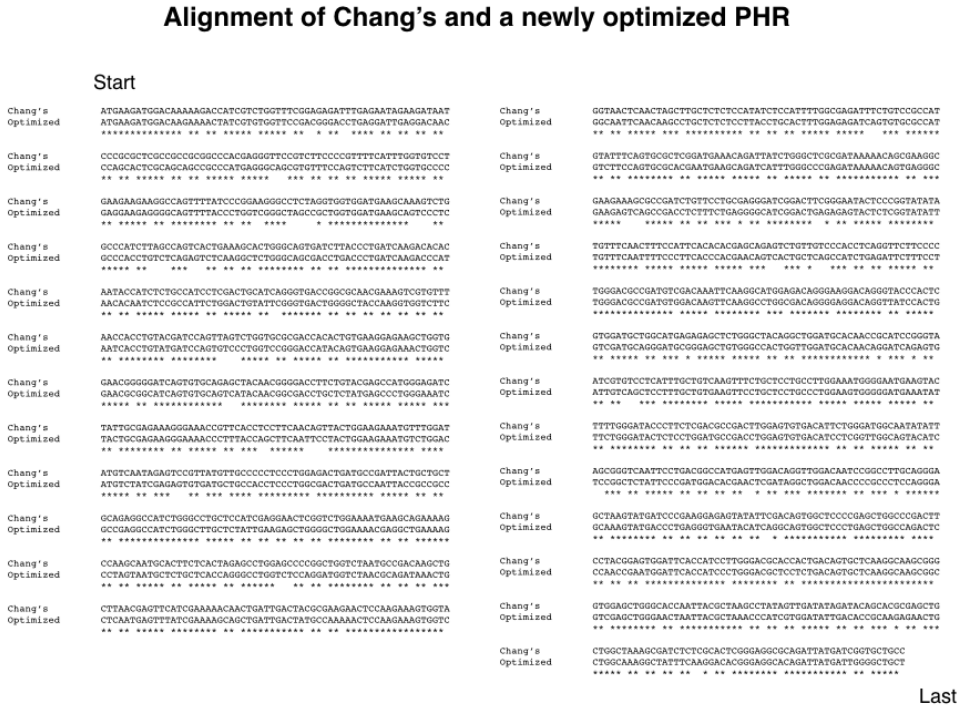

Supplemental Figure 2 Homology between original PHR and the newly optimized PHR.

Homology is 78% at nucleotide level.

Supplemental Fig. 3

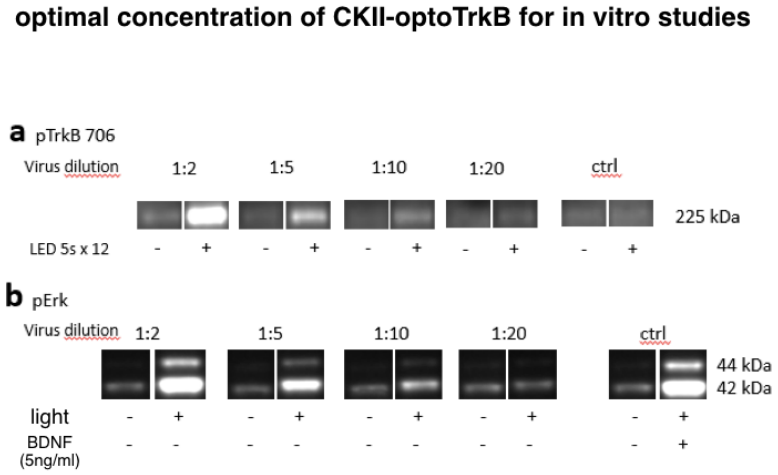

Supplemental Figure 3 Optimal concentration of CKII-optoTrkB for in vitro studies. Initial virus titer expressed as concentration of p24 protein: 8.37×10^7pg/ml. (a) Phosphorylation of Y706 site of optoTrkB and (b) phosphorylation of Erk after LED light exposure in primary cortical cells infected with different concentrations of lentivirus. To obtain different concentrations, the virus was diluted in sterile PBS to reach 1:2, 1:5, 1:10 and 1:20 dilutions. The virus was diluted just before administering it to the cells.

Supplemental Fig. 4

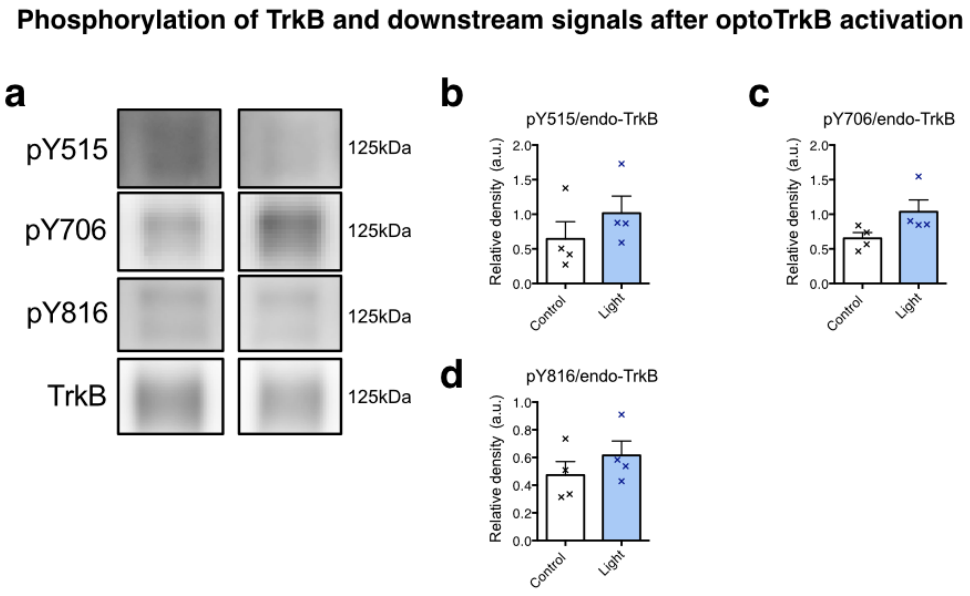

Supplemental Figure 4 Phosphorylation of endogenous TrkB after light stimulation. (a) Immunoblotting and quantitative analysis of phosphorylation at pY515, pY706, and pY816 sites after light stimulation (12 times for 5 seconds with 1-minute interval) (N = 4, each group). The intensity of endogenous TrkB phosphorylation (125 kDa, left panel) was normalized with the non-phosphorylated version of the same protein. (b-d) There was no significant effect of light exposure on phosphorylation of endogenous TrkB (unpaired t-test: pY515 p = 0.3289; pY706 p = 0.0889; pY816 p = 0.3576).

Supplemental Fig. 5

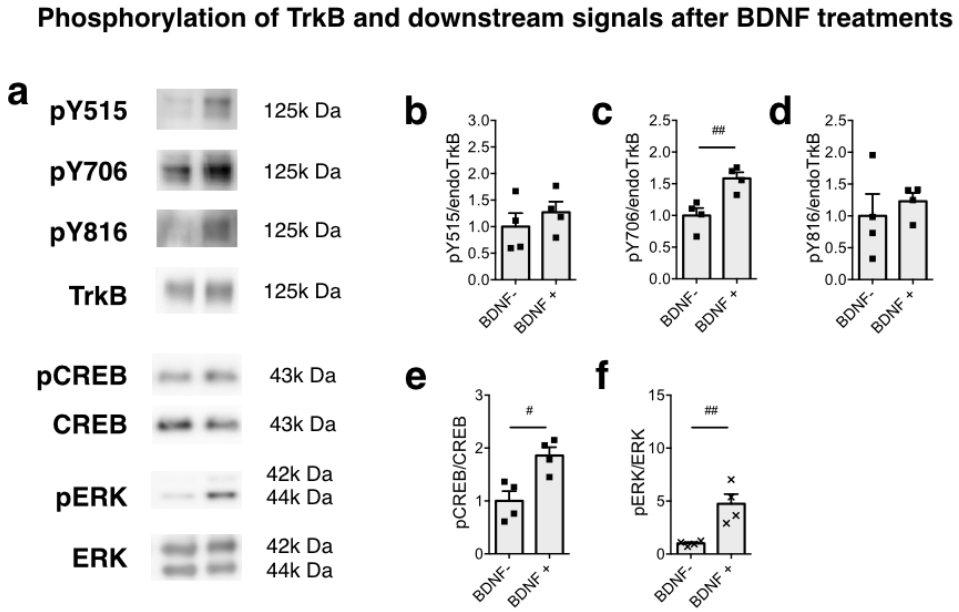

Supplemental Figure 5 Phosphorylation of TrkB and downstream signals after BDNF treatments in non-infected cultured cortical neurons. (a) Representative images of blotting for phosphorylated and non-phosphorylated endogenous TrkB. the ratio between phosphorylated/non-phosphorylated endogenous TrkB expression at Y515 (b), Y706 (c), Y816 (d), CREB (e), and ERK (f). Unpaired t-test showed that BDNF induced a significant phosphorylation of the Y706 site of TrkB receptor (pY706 $p = 0.0084$; pY816 = 0.5558; pY515 $p = 0.4345$) as well as phosphorylation of CREB and Erk (pCREB $p = 0.0120$; pErk $p = 0.0070$) # $p < 0.05$, ## $p < 0.01$. Bars represent means ± SEM.

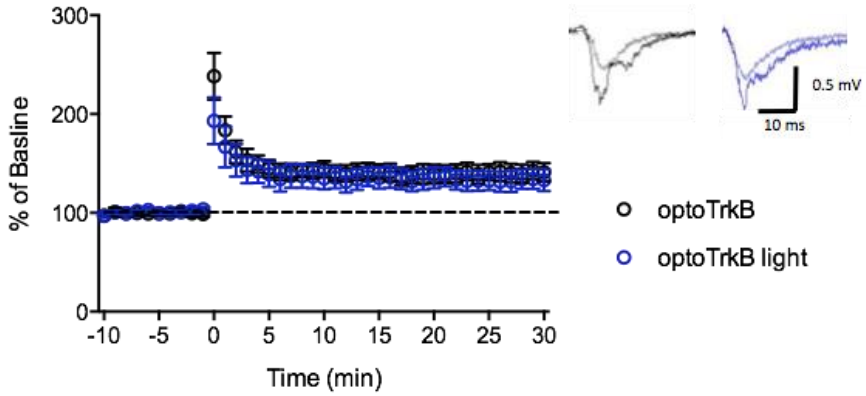

765

766 **Supplemental Figure 6** Enhanced neural plasticity after optoTrkB activation ex vivo.

767 The slices from CKII-optoTrkB infected mice were activated by light for 30 seconds. After 30 minutes, a long-term
768 potentiation (LTP) was induced by tetanic stimulation (100 pulses at 50 Hz). At 20 to 30 minutes after tetanization,
769 fEPSPs were larger than baseline in both non-light and light groups and there was no significant difference between
770 the groups (two-way ANOVA, $p = 0.0840$). Pictures in the right panel show representative traces of fEPSC during
771 baseline and after LTP induction. (optoTrkB, N = 6; optoTrkB light, N = 6). Error bars indicate mean ±SEM.

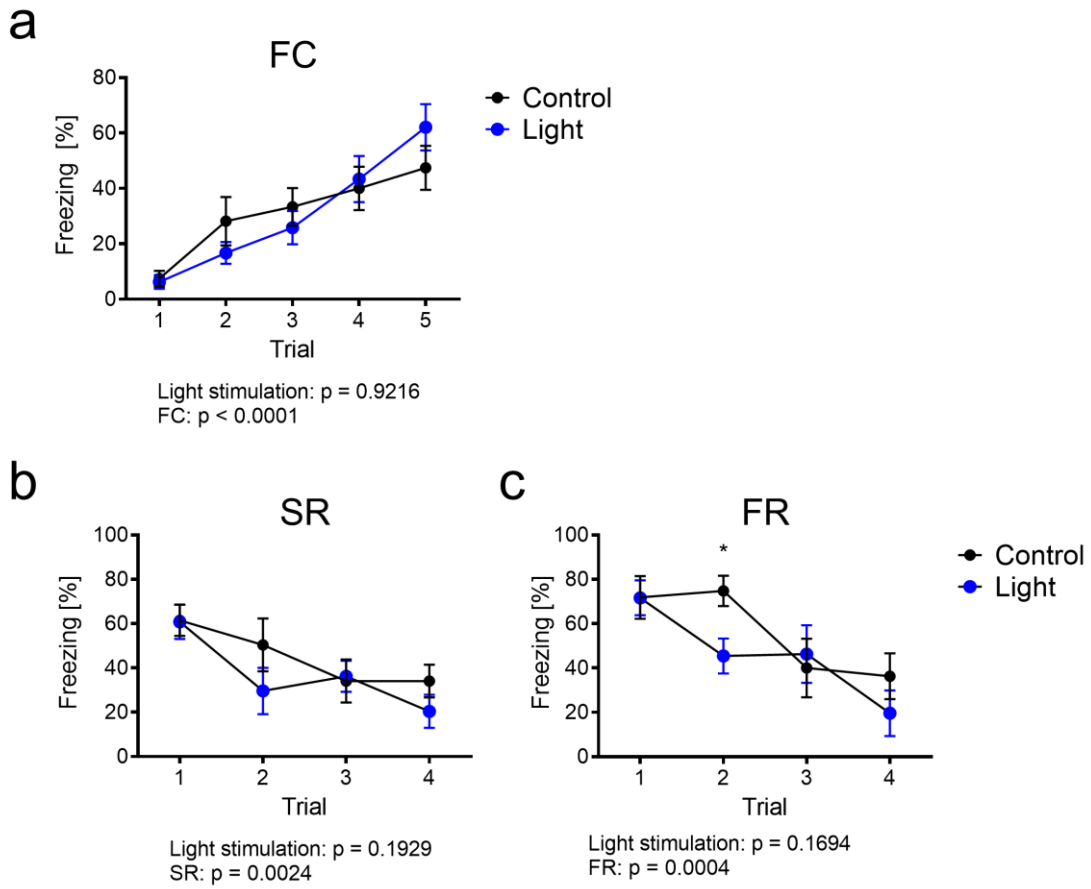

772

773 **Supplemental Figure 7**. Fear extinction paradigm with mice carrying optoTrkB with extinction training (a) Both
774 control (CKII-optoTrkB infected mice) and light groups (CKII-optoTrkB infected LED-exposed mice) increased
775 freezing during the conditioning/acquisition phase (two-way ANOVA, $p < 0.0001$) and exhibited the same levels of
776 fear acquisition. Spontaneous recovery (SR) (b) and fear renewal (FR) (c) after activation of CKII-optoTrkB during
777 fear extinction trainings. Previous light stimulation had no effect on freezing duration in SR (two-way ANOVA, $p =$
778 0.1929) or in FR ($p = 0.1694$). There was a significant difference in the 2nd session between control and light-
779 stimulated mice (post hoc: $p = 0.0454$). N = 8 per group. SR, spontaneous recovery; FR, fear renewal. * $p < 0.05$, **
780 $p < 0.01$. Error bars indicate mean ± SEM.

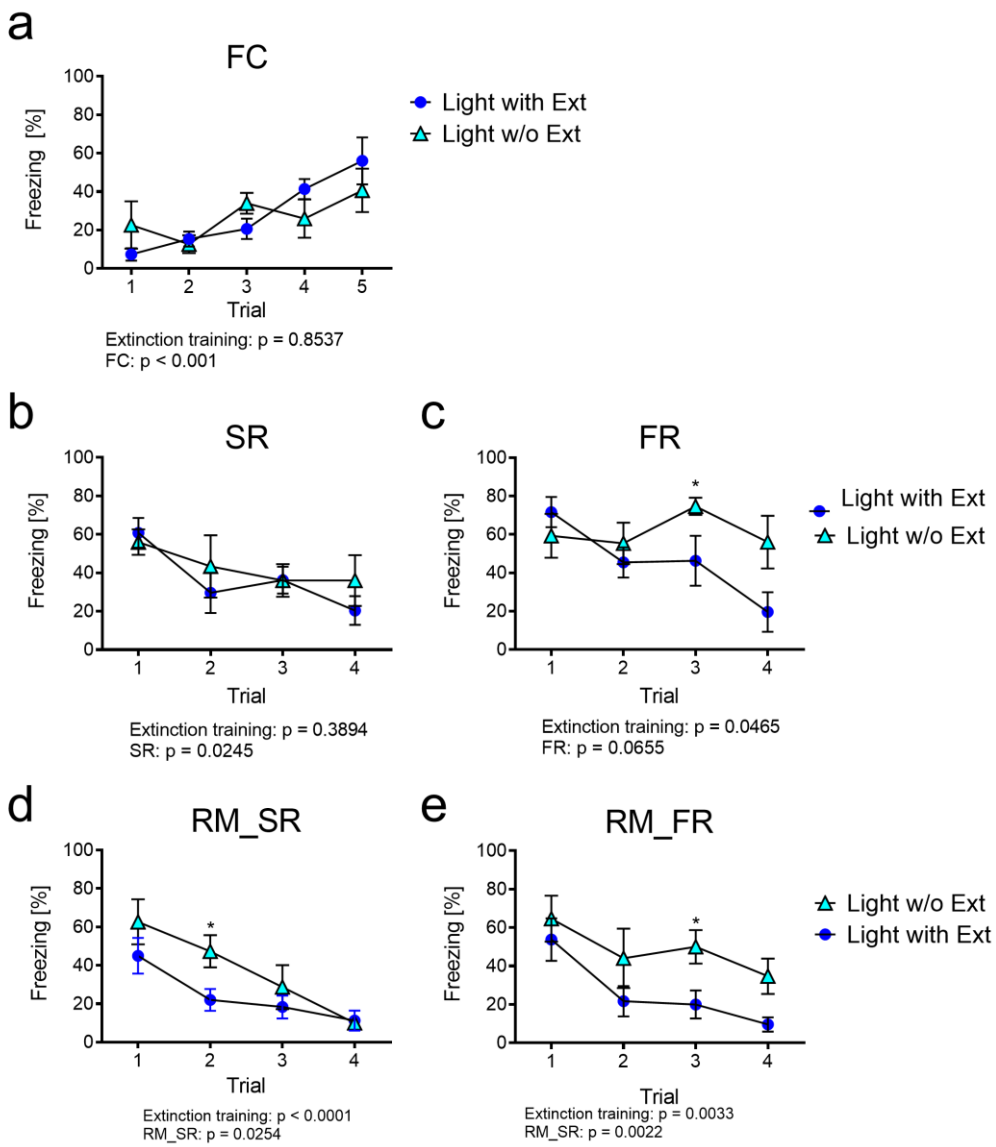

Supplemental Fig. 8: Comparison between groups exposed to light with and without extinction training. (a) Both the light group (CKII-optoTrkB-infected mice stimulated by light with extinction training) and the light group without extinction (CKII-optoTrkB-infected mice stimulated by light without extinction training) increased freezing during the conditioning/acquisition phase (two-way ANOVA, $p < 0.001$) and exhibited the same levels of fear acquisition. There was a significant decrease in FR (two-way ANOVA, $p = 0.0465$) (c), but not SR ($p = 0.3894$) (b) in the group with extinction training compared to the one without extinction training. The light with extinction group showed a stronger decrease in remote spontaneous recovery (RM_SR) ($p < 0.0001$) (d) and remote fear renewal (RM_FR) ($p = 0.033$) compared to Light w/o Ext (e). optoTrkB light, N = 8; optoTrkB light w/o extinction, N = 5) * $p < 0.05$, ** $p < 0.01$.

Supplemental table1 List of antibodies

Name	Application	Host	Dilution	Company	Product No
Horse Radish Peroxidase conjugated Goat Anti-Rabbit	WB	Goat	1:10000	BIO-RAD	#1705045
Horse Radish Peroxidase conjugated Goat Anti-Mouse	WB	Goat	1:10000	BIO-RAD	#1705047
Mouse anti-GFP	IHC	Mouse	F7 (1:625) C8 (1:667)	Memorial Sloankettering Monoclonal Antibody	04: clone19F7 02: clone19C8
Chicken anti-MAP2	IHC	Chicken	1:5000	Abcam	ab11267
Mouse anti-CAMKII	IHC	Mouse	1:500	Abcam	ab22609
Rabbit anti-FosB	IHC	Rabbit	1:500	Santa Cruz	sc-7203
Chicken anti-GFP	IHC	Chicken	1:1000	Abcam	ab13970
Alexa 546 Goat anti-mouse	IHC	Goat	1:400	LifeTechnologies	A21123
Alexa 647 Goat anti-chicken	IHC	Goat	1:400	LifeTechnologies	A21449
Alexa 546 Donkey anti-rabbit	IHC	Donkey	1:500	Thermo Fisher	A10040
Alexa 647 Donkey anti-mouse	IHC	Donkey	1:500	Thermo Fisher	A31571
Alexa 488 Donkey anti-chicken	IHC	Donkey	1:500	Jackson	AB_2340375

WB: Westernblotting
IHC: Immunohistochmistry

791

Supplemental table 2 Primers for Gibson cloning

Name	Sequence
fTrkB_link_R2	ctacccctccgccGCCTAGGATATCCAGGTAGAC
link_oPHR_F2	tcctaggcggcggaggggtagcggcggaggggttccgggggaATGAAGATGGACAAGAAAACTATC
oPHR_CK_R2	tcaccatggtggcgaaAGCAGCCCCAATCATAATC
pfTrkB_CK_F2	agcgatccccgggtaggatccATGTCGCCCTGGCTGAAG

792